Charge Transfer Transitions in Neutral and Ionic Polypeptides: A Theoretical Study

Luis Serrano-Andrés*

Departamento de Química Física, Universitat de València, Dr. Moliner 50, Burjassot, E-46100 Valencia, Spain

Markus P. Fülscher

Department of Theoretical Chemistry, Chemical Centre University of Lund, P.O.B. 124, S-221 00 Lund, Sweden

Received: September 23, 2000; In Final Form: May 23, 2001

We report on the vertical electronic excitation spectra of neutral polypeptides and their radical ions. Model systems including tri-, tetra-, and octamers in an α-helix and β-sheet alike conformation are studied by various computational methods. The results allow us to assign the band centered at about 7.5 eV in the absoption spectra of proteins to charge transfer states. The calculations also support conclusions from recent experiments which propose charge transfer as a possible mechanism for photoinduced electron transfer in polypeptide cations.

1. Introduction

Electron transfer is fundamental to many processes in living cells and may involve charge dislocation over distances ranging from a couple angstroms up to about 20 Å.[1] The mechanistic origin of this process is an active field of research and often controversial. Various models have been proposed and debated. In particular, it appears difficult to obtain conclusive experimental evidence if electrons are transported as "free" particles or if charge displacement is instead tightly coupled to hydrogen or proton shifts. The interested reader is referred to relevant reviews[2−5] and references therein.

If the protein backbone is viewed as a chain of weakly coupled, well isolated, and localized π systems, then the neutral polypeptide can be expected to behave like an electric insulator. In recent years, however, Schlag and co-workers[6−9] studied spectroscopically small oligopeptide cations in gas phase and could observe migration of the positive charge. Moreover, Asher and co-workers[10,11] described electron transfers in neutral peptides from the terminal carboxyl group to neighboring peptide groups, and also efficient transfer of charge through polypeptide backbones has been reported to occur both in polychromophoric polypeptides[12,13] and in small peptides.[14] To bear new insight in these mechanisms, a detailed knowledge of the electronic structure of polypeptides as probed by various spectroscopic methods is of utmost importance. For these reasons, we investigated the electronic structure of numerous amides and peptides by means of ab initio quantum chemical calculations.

Previous CASSCF/CASPT2 results on single amides[15,16] determined, in accordance with most of the experiments, the electronic spectra of the peptide group as composed by the following excitations: a weak band close to 5.5 eV due to $n \rightarrow \pi^*$ (W) excitations, a strong band at 6.5 eV corresponding to the $\pi \rightarrow \pi^*$ (NV_1) transition localized at the peptide bond, and an intense band at high energies, above 9.0 eV, which can be characterized as the second $\pi \rightarrow \pi^*$ (NV_2) transition found in amides. We can safely summarize that the assignment of the W and NV_1 transitions in isolated amides is well established. In contrast, the character of the absorption bands between 7 and 8.0 eV in the electronic spectra of polypeptides is unsolved, in particular an intense absorption band observed in the absorption spectra of polyamides such as polyglycine, polyalanine or polyserine near 170 nm (7.3 eV).[17] In a previous study of short polypeptide models,[18] we interpreted the band in terms of charge transfer (CT) excitations involving charge translocation between neighboring peptide units. Earlier proposals relating the band to the NV_2 state[19] or to $n_O \rightarrow \sigma^*$ transitions[20] were ruled out. The changes of the absorption profile for proteins in β-sheet, α-helical, or random coil conformations were also reproduced by our calculations. Finally, we provided an explanation for the lack of the 7.5 eV band in the electronic spectra of nylons, because of the larger distance between neighboring peptide units in these systems.

Recent findings and proposals about efficient charge migration in polypeptides[7,9,10] require a theoretical rationalization which will strongly benefit from a deep knowledge of the electronic structure of the peptidic chain. The analysis has to be performed on realistic models such as at least small oligopeptides and has also to include the study of ionized systems, where the electronic gap between the ground and low-lying electronic excited states is dramatically decreased and electron transport is largely enhanced at low energies. For these reasons, one of the main goals of the present contribution is to extend previous studies on model amides and peptides and to theoretically characterize the electronic spectra of polypeptide fragments including up to eight units adopting β-sheet or α-helix alike conformations. In addition, we studied the excited states structure of cations and anions of model peptides at different conformations in order to shed some light onto the change in the electronic structure induced during electron transport processes. Both, ab initio and carefully calibrated semiempirical methods are employed in order to get a consistent and accurate description of the electronic states structure and transition properties of the polypeptidic backbone.

* To whom correspondence should be addressed

10.1021/jp0034473 CCC: $20.00
Published on Web 08/24/2001

2. Methods

Multiconfiguration perturbation theory has developed into a very powerful tool to study electronically excited states of small molecules. Especially, the CASPT2[21,22] approach, which is based on a complete active space (CAS)SCF reference function,[23,24] has been successfully applied to a broad range of difficult problems in transition-metal chemistry and photochemistry.[25−27] Here, this approach is applied to study vertically excited states of dipeptides and tripeptides using ground state geometries optimized at the MP2 level of approximation. These results were used to carefully calibrate calculations on larger systems—tetra- and octapeptides—using more approximate approaches. To this end, three combinations of methods were used:

(i) As mentioned above, the ground-state geometries of the smallest model systems, the di- and tripeptide in α-helix or β-sheet alike conformations, have been optimized at the MP2/6-31G* level of approximation. To prevent large distortions from the experimentally observed protein structures, in all cases, the dihedral angles between the peptide groups, the so-called Ramachandran angles Ψ and Φ, were restricted to ideal values: $\Phi = 120°$ and $\Psi = -120°$ for antiparallel β-sheet and $\Phi = -57°$ and $\Psi = -47°$ for α-helix alike conformations. The vertically excited electronic states were then computed by the CASSCF/CASPT2 approach using atomic natural orbital (ANO) type basis sets[28] contracted to the following structure: C,N[3s2p1d]/H[2s]. The CASSCF reference functions included for each peptide unit three π orbitals (two occupied and one virtual) and the oxygen lone pair orbital. To remove weakly interacting intruder states from the CASPT2 wave functions, we applied the levelshift[29] technique using a shift of 0.3 hartree. Finally, transition dipole moments were calculated by the CASSCF state interaction (CASSI) method.[30]

(ii) Current hard- and software limitations prevent us from computing vertically excited states using the CASSCF/CASPT2 method for model systems larger than a tripeptide. For these reasons, we were seeking more approximate methods. Pilot calculations indicated that the CNDO/S method using the Mataga−Nishimoto electron−electron repulsion integral parameters[31] provide the most consistent results as compared to the CASSCF/CASPT2 results. To calibrate the CNDO/S method we therefore repeated the calculations on the small systems using the same geometry as that above.

(iii) Geometry optimizations at the MP2/6-31G* level of approximation become very expensive for systems of the size of an octapeptide. Therefore, we attempted to reduce the computational costs using the Merck force field to find the minimal energy structure. However, to prevent the results from being biased toward small model systems, we proceeded in a somewhat different way. For the antiparallel β-sheet structure, four polyglycine chains in antiparallel position, containing 24 peptide units, were first optimized using the Merck potential (the aforementioned constraints also apply). Likewise, for the α-helix structure, a polyglycine chain containing 24 peptide units was optimized using the Merck potential. Fragments of appropriate size were then cut out from the middle of the system and their extremes completed with hydrogen atoms placed at a distance of 1.1 Å. Here too, we first investigated the influence of the geometry on the vertical excitation energies of the small model peptides before proceeding to the tetra- and octapeptide fragments.

All ab initio calculations were performed using the MOLCAS version 4 software package,[32] except for the MP2 optimizations for which we used the Gaussian program.[33] The molecular mechanics minimizations (Merck potential) employed the SPARTAN code.[34] Finally, the CNDO/S calculations were carried out using the ZINDO program.[35]

3. Results and Discussion

3.1. Neutral Dipeptides and Tripeptides. The electronic absorption spectrum of the isolated peptide unit[15,16] can be rationalized in terms of a four orbital model, that is, the two doubly occupied π orbitals, π_1 and π_2, the lone pair orbital localized at the oxygen atom, n_O, and the antibonding π^* orbital, π_3^*. The model implies that the electronic absorption spectrum of a peptide unit is due to transitions of the type $n_O \rightarrow \pi_3^*$, $\pi_2 \rightarrow \pi_3^*$, and $\pi_1 \rightarrow \pi_3^*$. These valence excited singlet states are labeled W, NV_1, and NV_2, respectively. The $n_O \rightarrow \pi_3^*$ transition is observed at energies about 5.5 eV (shifted to 5.8−5.9 eV by solvent effects[17,20]) above the ground state and is characterized by a weak oscillator strength. The intense absorption maxima at about 6.5 eV is due to the $\pi_2 \rightarrow \pi_3^*$ excitation, whereas the $\pi_1 \rightarrow \pi_3^*$ transition is observed in the far UV at about 9.5 eV. In addition, especially in gas phase, one may also observe some very weak $n \rightarrow \sigma^*$, $\sigma \rightarrow \pi^*$, and a number of Rydberg states, labeled R_1, R_2, etc., in order of increasing energies.

In a previous paper,[18] we reported on the vertical electronic excitation spectrum of *N*,*N*-dimethylformamide. It was shown that a group of peaks centered at 7.7 eV were characteristic of states of Rydberg character. These assignments are in close agreement with experimental data but conflict the common assumption[19,36] that the 7.5 eV band in polypeptides is related to the NV_2 band of the isolated peptide group. Therefore, we proposed recently[18] that the 7.5 eV band is due to charge-transfer transitions between neighboring peptide units. Our calculations on a dipeptide model at different conformations followed the intensity patterns indicated by the experiment: the weak 5.5 eV (W) and intense 6.5 eV (NV_1) bands proved conformationally independent (localized on the isolated peptide unit), whereas the intensity of the 7.5 eV band depended strongly on the conformation. For instance, in polypeptides with random-coil structure, the NV_1 band carries most of the intensity, whereas the intensity of the 7.5 eV band increases for polypeptides adopting an α-helical structure.[17,37]

In the present paper, we shall extend previous calculations to larger systems. In a first step, we intend to calibrate the methods. Tables 1 and 2 compile the results obtained using different strategies for the model systems: $CH_3-(CONH-CH_2)_x-H$, with $x = 2$ (dipeptide) and $x = 3$ (tripeptide), see Figure 1 and ref 18. The two most usual conformations were included in the study: antiparallel β-sheet and α_R-helix alike structures. The geometries were obtained as explained in the previous section.

To analyze these results, consider the orbital diagram for two weakly interacting peptide units shown in Figure 2. Peptide units are enumerated in ascending order starting from the carboxyl and ending at the amino end. As indicated by the left and right half of the picture, we may expect to find W(*n*), $NV_1(n)$, and $NV_2(n)$ single excitations localized at peptide unit *n*. In addition, we may also find charge-transfer bands due to the displacement of electronic charge between neighboring peptide units. For instance, the CT_{12} charge-transfer excitation can be characterized as a one-electron promotion from the π_2 orbital of group 1 to the π_3^* orbital of group 2. In contrast, the CT_{O12} state involves charge transfer from the lone-pair orbital of the oxygen of the peptide group 1 to the π_3^* orbital of the peptide group 2.

TABLE 1: Computed Excitation Energies (ΔE, eV) Oscillator Strengths (f) of Two Model Polypeptides (See Figure 1) in the Antiparallel β 1-Strand Conformation[a]

CNDO/Merck		CNDO/MP2		CASPT2/MP2		
ΔE	f	ΔE	f	ΔE	f	state[b]
			Dipeptide			
3.66	0.001	3.64	0.001	5.63	0.001	W_1
3.65	0.001	3.65	0.001	5.57	0.001	W_2
6.60	0.093	6.62	0.159	6.14	0.204	$NV_1(2)$
6.73	0.697	6.77	0.626	6.20	0.444	$NV_1(1)$
7.21	0.034	7.23	0.048	6.87	0.148	CT_{12}
8.31	0.018	8.30	0.007	8.22	0.001	CT_{o12}
8.33	0.055	8.25	0.037	8.70	0.102	CT_{o21}
8.10	0.003	8.10	0.022	8.94	0.015	CT_{21}
			Tripeptide			
3.63	0.001	3.63	0.002	5.54	0.002	W_2
3.67	0.001	3.68	0.001	5.59	0.002	W_3
3.65	0.000	3.63	0.000	5.68	0.001	W_1
6.75	0.996	6.78	0.884	6.20	0.270	$NV_1(2)$
6.55	0.108	6.57	0.119	6.27	0.305	$NV_1(3)$
6.65	0.053	6.67	0.147	6.29	0.362	$NV_1(1)$
7.12	0.048	7.14	0.070	6.59	0.277	CT_{12}
7.25	0.032	7.28	0.045	7.12	0.031	CT_{23}
8.00	0.002	8.00	0.020	7.82	0.014	CT_{o12}
8.24	0.011	8.28	0.008	7.90	0.006	CT_{o32}
8.18	0.029	8.14	0.006	8.29	0.001	CT_{32}
8.14	0.007	8.12	0.023	8.78	0.004	CT_{o23}

[a] Merck or MP2 geometries and CNDO/S or CASPT2 methods employed. See text. [b] See Figure 2 and text.

TABLE 2: Computed Excitation Energies (ΔE, eV) Oscillator Strengths (f) of Two Model Polypeptides (See Figure 1) in the α_R-Helix Conformation[a]

CNDO/Merck		CNDO/MP2		CASPT2/MP2		
ΔE	f	ΔE	f	ΔE	f	state[b]
			Dipeptide			
3.63	0.001	3.57	0.001	5.24	0.001	W_1
3.58	0.001	3.55	0.001	5.28	0.002	W_2
6.64	0.171	6.81	0.164	6.00	0.170	$NV_1(2)$
6.76	0.451	7.00	0.497	6.07	0.261	$NV_1(1)$
7.54	0.002	7.58	0.009	7.27	0.146	CT_{o12}
7.80	0.066	7.85	0.028	7.46	0.020	CT_{12}
7.42	0.030	7.51	0.042	7.74	0.122	CT_{o21}
7.97	0.064	8.00	0.112	7.80	0.010	CT_{21}
			Tripeptide			
3.64	0.001	3.53	0.001	5.24	0.001	W_3
3.57	0.001	3.61	0.001	5.46	0.001	W_2
3.59	0.001	3.59	0.001	5.29	0.001	W_1
6.57	0.128	6.65	0.150	5.87	0.205	$NV_1(3)$
6.69	0.308	6.76	0.477	5.94	0.178	$NV_1(2)$
6.72	0.438	6.97	0.305	6.10	0.304	$NV_1(1)$
7.45	0.004	7.28	0.006	6.60	0.041	CT_{o31}
7.56	0.008	7.52	0.016	6.78	0.032	CT_{31}
7.34	0.013	7.56	0.014	6.83	0.080	CT_{o21}
7.50	0.018	7.68	0.093	7.21	0.154	CT_{o32}
7.56	0.008	7.81	0.005	7.87	0.006	CT_{21}
7.72	0.096	7.93	0.024	7.93	0.032	CT_{32}

[a] Merck or MP2 geometries and CNDO/S or CASPT2 methods employed. See text. [b] See Figure 2 and text.

Finally, the opposite charge-transfer excitations from group 2 toward group 1 may also be observed. The two types of CT transitions will be labeled hereafter: CT_1 ($\pi \rightarrow \pi^*$) and CT_2 ($n \rightarrow \pi^*$), provided this distinction is possible. The ordering of the CT states can be understood qualitatively by geometric arguments and considering the localization of the orbitals; that is, the distance between the N(2) atom and the C(1)O(1) group is larger than the distance between N(1) and C(2)O(2) (cf. Figure 1). Other excitations involving the $\pi_1$orbitals would be found

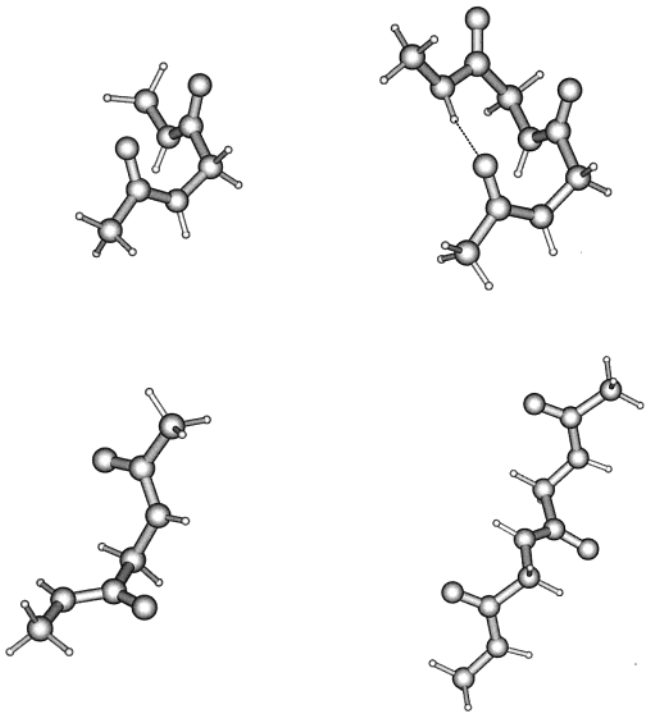

Figure 1. Structures of the dipeptide and tripeptide models (polyglycine with terminal methyl groups) employed in the present calculations, at the α-helix (top) and antiparallel β-sheet (bottom) conformations. The most important hydrogen bonds are indicated in the picture. The labeling of the peptide unit (1, 2, and 3) begins by the peptide linked to the terminal methyl group by the CO side.

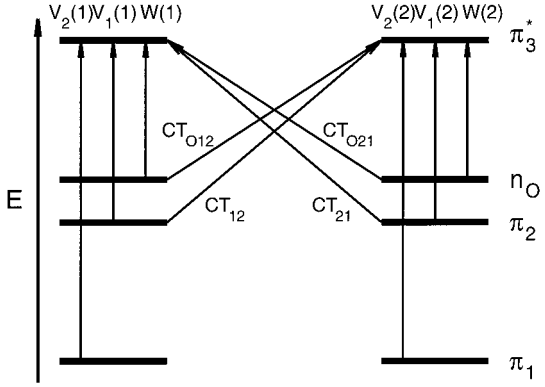

Figure 2. Orbital scheme and single excitations in a two-peptide system. See text for explanation.

at much higher energies. We focus our attention on the W and NV_1 bands localized at the individual peptide groups as well as on the CT_1 and CT_2 excitations. When relating the present scheme to actual models, two considerations are relevant. First, the nature of the localized transitions, W and NV_1, is basically independent of the conformation. In contrast, the charge transfer states, which involve at least pairs of neighboring peptide groups, have such a mixed character that a correlation between intensity and conformation might be difficult to establish.[18] Second, in a model such as a dipeptide, the amide units are not equivalent because of the different attachment of the alkyl groups (through N or C), and therefore, the corresponding pairs of charge transfer transitions lie at different energies. In a real polyamide, however, the peptide groups in the middle of the chain are basically equivalent and the different charge transitions have cooperative effects. Moreover, additional transitions can be expected when α-helix or β-sheet conformations are con-

sidered, because the number of neighboring (but not consecutive) peptide groups largely increases.

Turning back to the inspection of the CASSCF/CASPT2 results in Tables 1 and 2, we note that the W(n) states are almost degenerate and computed with excitation energies ranging from 5.2 to 5.5 eV for the β-strand conformation and 5.5 to 5.7 eV for the α-helix conformation. All W(n) states are characterized by small oscillator strengths. This is typical for $n \rightarrow \pi^*$ transitions in aromatic systems, where the overlap between the lone pair and the π orbitals is almost negligible. The valence excited $NV_1(n)$ states are predicted to follow the W bands. The computed vertical excitation energies range from 6.1 to 6.3 eV for the models of an antiparallel β strand and from 5.9 to 6.1 eV for the models of an α helix. The computed oscillator strengths range from 0.17 to 0.44. Finally, the $NV_1(n)$ excitations are followed by a series of charge transfer states. Because of the elongated structure of the models representing an antiparallel β strand, we find only CT states involving nearest neighbors. In contrast, the tripeptide model of an α helix includes also CT states involving next nearest neighbors. In general, the computed oscillator strengths of the CT states are less than 0.05. However, for each of the models, we also find one CT state which has a remarkably large oscillator strength (≈0.15). The predicted excitation energies of the intense CT are ≈6.8 and ≈ 7.2 eV for an antiparallel β strand and α helix, respectively. To summarize, the excitation energies of the models representing an α helix are predicted to have somewhat lower excitation energies and oscillator strengths than those of the models representing an antiparallel β strand. All following transitions have been computed with energies much higher than 9.0 eV and have not been included here.

The W(n) transitions can undoubtedly be assigned to the weak 5.7−5.8 eV band described in the solution spectra of polypeptides,[17,20] which are shifted to higher energies because of solvation effects. The assignment of the $NV_1(n)$ transitions to the prominent band observed in the electronic spectra of polypeptides at 6.4−6.7 eV with high intensity is also straightforward. This is the band typically observed for all peptides ranging from small amides[15,38] to large polymers such as nylons.[20] The band follows the additivity rule[19] and was shown to be insensitive to conformational changes.[17,18] The present calculations strongly suggest that the intense band with a maximum at about 7.5 eV observed for polypeptides in aqueous solutions should be assigned to CT states. As indicated by the change of energy and intensity of the most intense charge CT states for the various model systems, this band is, in accord with experiment,[17] computed to be sensitive to conformational changes.

By application of the exciton theory[39] it was predicted that the NV_1 band of helical polypeptides should split into two components polarized in perpendicular directions. Similarly, the W band was also predicted to be composed of two components. The splitting has been confirmed by experiment.[20] Our calculated polarization directions are in agreement with the predictions of the exciton theory; that is, in the α-helix dipeptide model, the polarization angles of the near degenerate pairs of NV_1transitions are +64° and −25° for the $NV_1(2)$ and $NV_1(1)$ bands, respectively, with respect to the inertial axes of the molecule. The present calculations also predict that the intense CT bands are polarized in a direction perpendicular to the axis of the chain and parallel to the C═O bond. In planar systems, these transitions are obviously polarized in the plane of the polypeptide chain. For α-helical structures, the intense CT transitions are polarized along the axis of the helix. These polarization directions are compatible with experimental information[40] and led Robin[20] to the assumption that the 7.5 eV band observed in electronic spectra of proteins is due to a $n \rightarrow \sigma^*$ transition. However, Robin's assignment is unlikely to explain the intensity of the 7.5 eV band, whereas the CT bands carry a substantial fraction of intensity.

The present results compare well with those obtained in a previous CASSCF/CASPT2 study[18] for the dipeptide model: A total of 15 conformations was studied by changing systematically the Ramachandran angles Ψ and Φ, whereas the geometry of the peptide units was not optimized. We find, in general, that unlike the W and NV_1 bands the energy and intensity of the CT bands depend strongly upon the conformation of the system. For polypeptides in a β-sheet conformation, the absorption bands with mamxima at 6.3 and 7.5 eV are approximately of similar intensity. In contrast, the calculations predict for polypeptides in a α-helical conformation that the charge-transfer transitions tend to increase their relative intensities.

To support the interpretation of the electronic spectra of polypeptides given in the previous paragraphs, it is important to study even larger model systems and to include hydrogen bonding interactions. Such calculations are, however, beyond the limits of accurate ab initio methods. Other methodologies, in particular DFT-based methods for excited states, were tested and discarded because of their poor treatment of charge-transfer transitions.[41] For these reasons, we decided to use the semiempirical CNDO/S method in combination with geometries optimized using molecular mechanics. The CNDO/S approach was selected from the manifold of semiempirical methods because it better matched the present ab initio results.

Tables 1 and 2 include also the results obtained by the CNDO/S method using two sets of geometries: first, the excitation energies and oscillator strengths for the geometries determined at the MP2 level of approximation and, second, using the Merck structures. By inspection, we find that the geometry has only a small effect on the computed excitation energies. In general, the differences are less than 0.15 eV, except for CT transitions in the tripeptide model adopting an α-helical structure for which the largest deviations increase to 0.25 eV. Comparing the results obtained by the CNDO/S and CASSCF/CASPT2 method we find that the semiempirical method underestimates the excitation energies for the W(n) states by ≈1.8 eV and overestimates the excitation energies of the $NV_1(n)$ states by ≈0.5 eV. The CASSCF/CASPT2 method is, however, also known to underestimate the valence $\pi \rightarrow \pi^*$ excitations in large molecules.[42] Hence, the correction should be somewhat smaller (≈0.2 eV). The deviations in the CT transitions are less systematic. In general, the excitation energies obtained using the CNDO/S method are overestimated with respect to the CASPT2 results. In some cases, however, we also find that the excitation energies are underestimated. The difference range from about −0.8 to +0.8 eV. Considering also the CT transitions involving intermediate groups of the tripeptide model, it can be concluded that the correction needed to adjust the excitation energies obtained by the CNDO/S method to the CASPT2 results is 0.2 eV and of the same size as for the NV_1 transitions. The oscillator strengths obey, in general, the trends computed at the CASSCF/CASPT2 level of approximation: The intensities of the NV_1transitions are the strongest and appear to be somewhat overestimated. The intensities of the CT transitions are in general lower in the semiempirical approach. The relative weighting of the various CT transitions is also different as compared to the CASSCF/CASPT2 method.

TABLE 3: Computed and Experimental Excitation Energies (ΔE, eV) and Oscillator Strengths (f) of Several Polypeptides in the Antiparallel β-Sheet Conformation (cf Figure 2)

theoretical				
CNDO[a]	cCNDO[b]			exp[c]
ΔE	ΔE	f	band	ΔE
		Tetrapeptide (1 Stranded)		
3.6−3.7	5.4−5.5	0.004	W	5.9
6.5−6.7	6.3−6.5	1.530	NV_1	6.2−6.5
7.1−7.3	6.9−7.1	0.120	CT_1	7.2−7.5
8.0−8.4	7.8−8.2	0.223	CT_2	
		Octapeptide (1 Stranded)		
3.6−3.7	5.4−5.5	0.009	W	5.9
6.5−6.8	6.3−6.6	2.999	NV_1	6.2−6.5
7.1−7.3	6.9−7.1	0.300	CT_1	7.2−7.5
8.0−8.4	7.8−8.2	0.513	CT_2	
		Octapeptide (2 Stranded)		
3.6−3.7	5.4−5.5	0.003	W	5.9
3.7−3.8	3.5−3.6	0.008	W_{H-bond}	
6.4−6.5	6.2−6.3	1.199	$NV_{1H-bondinH}$	6.2−6.5
6.6−6.7	6.4−6.5	1.637	$NV_{1H-bondinO}$	
6.8−7.0	6.6−6.8	0.468	$CT_{1H-bond}$	
7.3−7.4	7.1−7.2	0.032	$CT_{1nonH-bond}$	7.2−7.5
7.4−7.7	7.2−7.5	0.001	$CT_{throughH-bond}$	
≫7.8	≫7.6		Higher CT	

[a] CNDO/Merck results. [b] Corrected CNDO/Merck results. See text. [c] References 17 and 20. Spectra in solution.

The discussion presented above pretends that the CASSCF/CASPT2 method is "fail safe" and "accurate". Evidently, this is not the case. However, a large number of previous studies focusing on spectroscopically well characterized systems show that the computed excitation energies, in general, agree with the experimentally observed absorption band maxima with an accuracy of 0.3 eV or better.[27,43,44] In particular, we also like to refer the interested reader to the papers investigating the spectroscopic properties of amides and the isolated peptide unit.[15,16] Because of a lack of a large number of unambiguous experimental data, the accuracy of calculated transition dipole moments is more difficult to access. In general, we found computed and experimental transition directions to agree with an accuracy of about 20°. Finally, the relative oscillator strengths are found to confirm observations. The accuracy tends to be better for strong absorption bands.

3.2. Larger Neutral Polypeptides. Table 3 shows the results for the extended models representing a polypeptide in an antiparallel β-sheet alike conformation of which the first two are single stranded chains. The third model represent a fragment of a double stranded, antiparallel β sheet and thus allows for hydrogen bonding interaction between neighboring strands. The models are shown in Figures 3 and 4. Note that the oscillator strengths given in Table 3 are computed as the sum over all oscillator strengths of transitions belonging to a class. The geometries and methods follow the considerations made in the previous section.

The structure of the predicted absorption spectrum of the single-stranded polypeptides adopting an antiparallel β-sheet alike conformation is very similar to that found for the corresponding dimer and trimer models. States of W character are lowest in energy and weakest in oscillator strength. Next to these states we find a group of NV_1 states carrying most of the intensity. At energies ranging from 7.1 to 7.3 eV, the calculations predict a number of CT states which involve electron transfer between nearest neighbors and π orbitals only. States involving electron transfer from the lone pairs located at the oxygen atom to the antibonding π orbitals are found at energies above 8.0 eV. The sum of all oscillator strengths of the CT states is five times smaller than that of the NV_1 states but orders of magnitude larger than that of the W states. If the CNDO/S results are corrected according to the calibrations made with the CASSCF/CASPT2 method in the previous section, the excitation of the W bands energies should be increased by 1.8 eV (a deviation for the $n \rightarrow \pi^*$ transitions which has been usual in many semiempirical approaches) and the excitation energies of the $\pi \rightarrow \pi^*$ transitions (both NV_1 and CT bands) decreased by 0.2 eV, as it was discussed previously. The corrected CNDO/S values place the W bands in the single-stranded β-sheet peptides at 5.4−5.5 eV (in isolated media), the NV_1 transitions at 6.3−6.6 eV, and the CT transitions in two groups of bands at 6.9−7.1 eV and 7.8−8.2 eV, respectively. If two stretched polypeptide strands are brought together to form an antiparallel β-sheet alike structure, we cannot find any significant changes in excitation energies and oscillator strength of states of W and NV_1 character. In contrast, the hydrogen bonding interactions appear to shift the low energy CT states to the red and lead to an increase in oscillator strength. The result is a large number of excitations having each slightly different energies and properties depending upon the intrapeptide and hydrogen bonding interactions. In the spectra, a single, broad band is expected to be observed as the result of collective excitations.

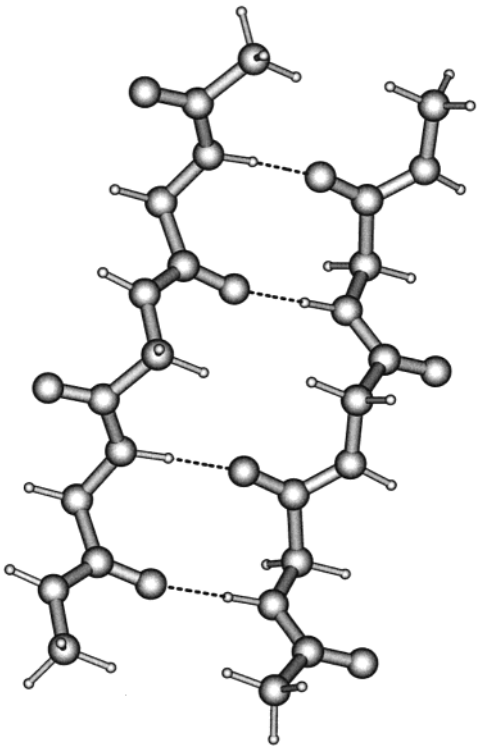

Figure 3. Structure of the two-strand antiparallel β-sheet system employed in the present calculations (eight total peptide groups involved). The one-stranded β systems include one single chain with the corresponding peptide units. The most important hydrogen bonds are indicated in the picture.

The results for the models including four or eight peptide units in a α-helical conformation are collected in Table 4, and the geometry of the larger model is shown in Figure 4. Here too, the differences between the "large" model systems and the corresponding dimer and trimer models are small. States of W character are predicted at energies ranging from 5.4 to 5.5 eV (CNDO/S corrected values) with very small oscillator strengths. As the model systems are enlarged to eight or more peptide units, hydrogen bonds between unit n and unit $n + 3$ can be

TABLE 4: Computed and Experimental Excitation Energies (ΔE, eV) and Oscillator Strengths (f) of Several Polypeptides in the α-Helical Conformation (cf Figure 3)

theoretical				
CNDO[a]	cCNDO[b]			exp[c]
ΔE	ΔE	f	band	ΔE
		Tetrapeptide		
3.6−3.7	5.4−5.5	0.0034	W	5.9
6.5−6.7	6.3−6.5	0.9507	NV_1	6.2−6.5
6.8−8.1	6.6−7.9	0.7018	CT	7.2−7.5
		Octapeptide		
3.6−3.7	5.4−5.5	0.0070	W	5.9
6.3−6.6	6.1−6.4	2.0180	NV_1	6.2−6.5
6.7−8.1	6.5−7.9	1.2295	CT	7.2−7.5

[a] CNDO/Merck results. [b] Corrected CNDO/Merck results. See text. [c] References 17 and 20. Spectra in solution.

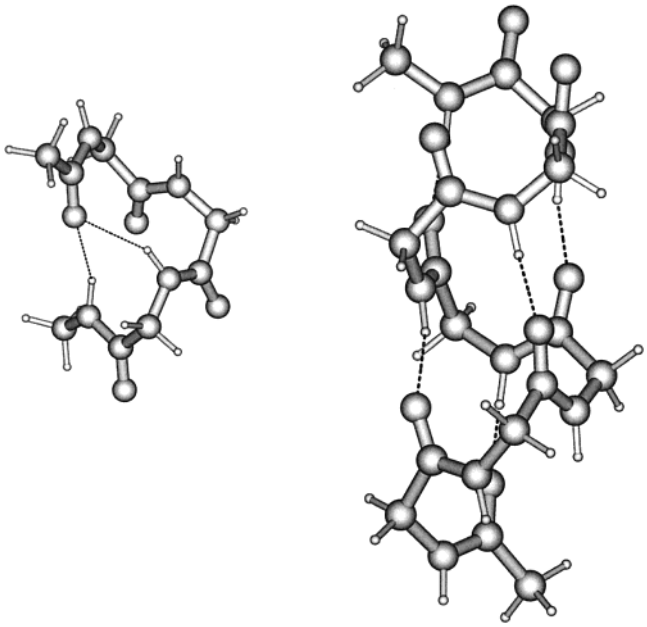

Figure 4. Structures of the tetrapeptide and octapeptide models (polyglycine with terminal methyl groups) employed in the present calculations at the α-helix conformation. The most important hydrogen bonds are indicated in the picture.

formed. Similar to the situation found for the antiparallel β sheet, the hydrogen bonding interaction is predicted to induce a red shift of the position of the NV_1 states (≈0.2 eV) and an increase of the concomitant oscillator strength. In contrast, the CT transitions are hardly affected by the hydrogen bonding interaction. We also find that the characterization of the CT state into subgroups such as hydrogen bond acceptors or donors and non-hydrogen-bonded groups is hardly possible. For these reasons, we collected all states into a single group only. If the excitation energies obtained at the CNDO/S level of approximations are corrected according to the rules given above we find an excellent agreement between theory and experiment: absorption maxima are predicted at energies close to 5.5, 6.1−6.4, and 6.7−8.1 eV.

The obtained overall results are in accord with the experimental measurements[17,20] for nonrandom coil polypeptides and follow the trends observed in shorter polyamides. The collective character of the high-energy charge-transfer band was already proposed some time ago,[40,45,46] when the 7.75 eV band measured in helical polypeptides with a parallel polarization was suggested to arise from constructive interferences between bands at shorter and longer wavelengths. It has to be concluded that the charge transfer band will be observed as a single feature which, on one hand, follows the additivity rule by summing up the contributions of the different peptide pairs, but, on the other hand, its intensity will strongly vary upon the conformational changes, as it was shown before.[18] From the obtained results, it is noticeable that some differences exist between the CT bands in the α-helical and β-sheet polypeptides (not in the W and NV_1 bands, which are conformationally independent), in particular that the relative ratio of intensities between the NV_1 and CT bands is much larger in the α-helical than in the β-sheet conformers. This fact is also in agreement with the experimental findings, where polypeptides in an α-helical conformation have been shown to increase the relative intensity of their charge-transfer transitions as compared to those of the β-sheet conformers.[17,20]

3.3. Ionized Polypeptides. The large energy gap of about 7.5 eV between the ground and CT states justifies the view of the protein backbone being an insulator. Radical ions are, however, known to have much lower excitation energies. In order for the electron transfer to be favorable initiated, and provided that the mechanism involves the peptide backbone, it seems plausible to think that the chain of peptides has to be viewed like a radical ion or a doped species. It has been recently observed that the photoinjection of positive charge at a specific chromophore in a series of polypeptides lead to facile migration of the charge over long peptide chains.[6−8] The evidence of electronic hole transfer indirectly supports our assignment on charge transfer states of neutral polypeptides. For these reasons, we also computed the vertically excited states of radical ions of the model peptides using the CASSCF/CASPT2 approach. Because none of the semiempirical methods available to us was found to be appropriate to reproduce CASSCF/CASPT2 results, we report only calculation on results for the di- and tripeptide models. Moreover, we also like to emphasize that the wave functions computed by the CASSCF/CASPT2 method are always proper spin functions.

In Table 5, we have collected the computed excitation energies and oscillator strengths for the radical cations of the di- and tripeptide models at the optimized structures of neutral α_R-helix and β-sheet systems. For the β-sheet structures and at low excitation energies, the charge hole is localized on the π orbitals. The state ordering π_{N1}, π_{N2}, and π_{N3} is somewhat superficial because they hardly could be identified in a very long chain. In particular, the energy difference 0.06 eV between states π_{N1} and π_{N2} represents clearly a near-degeneracy situation. At somewhat higher excitation energies, 0.5−0.9 eV, the charge hole is localized at the oxygens lone pair orbitals. Our calculations also predict that a photon of about 3 eV in energy is needed to promote the hole into the π_{CO} orbital. Finally, we find the first vertically excited-state involving a virtual orbital at an energy of 5.2 eV.

For the α-helix structures, the scheme of excitation energies is more complex. The difference can be explained taking into account that polypeptides with an α-helical conformation and more than two units form strong hydrogen bonds. In particular, we find large changes in excitation energies for the n_{O1} and π_{N1} states. Evidently, the corresponding orbitals are strongly perturbed as they are involved in the formation of the hydrogen bond with the N_3H group. Here too, promoting the hole into the π_{CO} orbital costs about 2.5−3 eV in energy.

Table 5 also includes the excitation energies and oscillator strengths for a model dipeptide cation at the equilibrium geometry of the cation. The latter has been optimized at the UMP2/6-31G* level of approximation. The positive charge is

TABLE 5: Excitation Energies (Δ*E*, eV) and Oscillator Strengths (*f*) of Polypeptide Radical Cations Computed at the CASSCF/CASPT2 Level[a]

β-Sheet Conformation						
dipeptide				tripeptide		
neutral geo.[b]				neutral geo.[b]		
Δ*E*	*f*	Δ*E*	*f*	Δ*E*	*f*	state
(9.31)[c]				(9.40)[c]		π_{N1}
0.31	0.013			0.06	0.047	π_{N2}
				0.41	0.001	π_{N3}
0.36	0.000			0.42	0.000	n_{O1}
0.47	0.004			0.74	0.000	n_{O2}
				0.85	0.000	n_{O3}
				2.46	0.002	π_{CO3}
2.92	0.003			3.13	0.003	π_{CO2}
3.13	0.036			3.03	0.040	π_{CO1}
5.20	0.004			5.36	0.004	$\pi_{N1}n_{O1},\pi_2^*$

α-Helix Conformation						
Dipeptide				Tripeptide		
Neutral geo.[b]		Cation geo.[d]		Neutral geo.[b]		
Δ*E*	*f*	Δ*E*	*f*	Δ*E*	*f*	state
				(8.99)[c]		π_{N3}
				0.22	0.002	n_{O3}
(9.18)[c]		0.18	0.000	0.69	0.007	π_{N2}
0.32	0.013	1.04	0.000	1.34	0.000	π_{N1}
0.40	0.001	(8.86)[c]		0.53	0.001	n_{O2}
0.45	0.005	1.34	0.000	1.19	0.001	n_{O1}
				2.89	0.025	π_{CO3}
3.20	0.012	3.20	0.001	3.67	0.001	π_{CO1}
3.04	0.021	3.67	0.003	3.27	0.002	π_{CO2}
5.33	0.016	5.51	0.016	5.32	0.000	$\pi_{N2}n_{O1},\pi_2^*$

[a] Transitions with respect to the cation ground state unless indicated. Neutral MP2 optimized geometries, otherwise indicated. [b] Neutral MP2 optimized geometries, otherwise indicated. [c] Lowest ionization potentials from the neutral system. [d] Radical cation (n_{O2}) UMP2/6-31G* optimized geometry.

TABLE 6: Excitation Energies (Δ*E*, eV) and Oscillator Strengths (*f*) of Dipeptide Radical Anions Computed at the CASSCF/CASPT2 Level[a]

β sheet		α helix		
Δ*E*	*f*	Δ*E*	*f*	state
(2.14)[c]		(1.75)[c]		π_2^*
0.46	0.053	0.34	0.040	π_1^*
2.88	0.006	5.35	0.013	$\pi_{N1}\pi_1^*\,\pi_2^*$
5.27	0.002	5.08	0.023	$n_{O1}\pi_1^*\,\pi_2^*$
5.47	0.019	5.18	0.002	$n_{O1}\pi_1^*\,\pi_2^*$
5.54	0.013	5.71	0.003	$n_{O2}\pi_1^*\,\pi_2^*$

[a] Transitions with respect to the cation ground state unless indicated. Neutral MP2 optimized geometries. [b] Neutral MP2 optimized geometries. [c] Lowest electron affinity from the neutral system.

then placed at the lone-pair orbital of the oxygen atom, which belongs to the CO group bridged to the internal CH_2 unit of the dipeptide, as the most favorable situation. The energy difference with respect to the next state is largely decreased to 0.18 eV. The absorption energies of the π_{CO} excited states remain larger than 3 eV.

Table 6 compiles the excitation energies and oscillator strengths computed for the radical anion dipeptide model at the α and β structures of the neutral system. A single empty orbital is available per peptide unit, and the energy difference between states with the electron localized on the neighboring unit is low: 0.34 and 0.46 eV, respectively. The second and higher excited states involve an excitation from an occupied orbital into the second empty π orbital. These states are placed at energies above 3 eV.

Considering the shift in excitation energies when going from the neutral molecule to its radical ions, we may expect the charge transfer states at very low energies. Evidently, we cannot expect the radical ion states to have the same electronic structure as the excited states of the neutral molecule. Nevertheless, one may compare the situations if one considers the localization of the orbitals. Baranov and Schlag[9] recently reported a theoretical study on a model dipeptide in which an efficient charge flowing mechanism is proposed to be led by the coupling of the low frequency amplitude torsions inherent to peptide motions. A hole hopping mechanism between local sites can be understood if the coupling is able to overcome local effects and create temporarily delocalized charge transfer states. The coupling should be strong enough to ensure high probabilities of charge transition during the time the molecule passes a favorable conformation, and it should be able to wash out small energy differences which are observed as local ionization potentials. The two localized situations, that is, the charge hole on the oxygen lone-pair orbital in one peptide or its neighbor, are nearly degenerate in energy when a full geometry optimization is performed for the model dipeptide at the UHF/6-31G* level (0.05 eV).[9] The same authors estimated upper bounds for the energy barriers of 0.4 eV between the two localized situations. The present calculations confirm this estimate. Furthermore, our results suggest that the "best hopping path" is strongly dependent on the secondary and tertiary structure of the protein. Our results also show that in polypeptides a larger number of states with very different character can be found in a rather narrow energy band. This situation is further strengthened by the ample conformations a polypeptide chain may adopt and the lifetime of an excited state. By computing the orbital energy difference of the HOMO and HOMO-1 orbitals at the transition state geometry, Baranov and Schlag[9] estimated a coupling constant of 0.18 eV between two localized situations. The energy difference is small enough to allow charge transfer through small torsions of the peptide units around the Φ and Ψ angles.

4. Summary and Conclusions

In this paper, we reported on the vertical electronic excitation spectra of neutral polypeptides and their radical anions. We used various computational tools, ranging from molecular mechanics force field methods to modern ab initio techniques. In particular, the CASSCF/CASPT2 method was used to study small model systems and to calibrate more approximate methods, such as the semiempirical CNDO/S approach. The systems investigated include di-, tri-, tetra-, and octamers in an α-helix and β-sheet alike conformation.

The calculations on the neutral model systems confirm our earlier predictions that the absorption band in UV/VIS spectra of proteins centered at about 7.5 eV is due to excited states which can be characterized as charge transfer states. Direct confirmation by experiment is not available. However, the present model is compatible with all experimental data at hand such as the polarization direction of the transitions and the dependence of the shape of the spectra on the conformation of the polypeptide.

Indirect support is also given by recent experiments on the charge transfer mechanism in polypeptide cations. The computed vertical excitation spectra of polypeptide radical ions show that at low excitation energies there is a large number of nearly degenerate electronic states of widely different character. In agreement with earlier calculations and experiments, we estimate

an energy barrier of about 0.4 eV to shift an electron hole from one peptide unit to its neighbor. Thus, after the primary step, the absorption of a photon, the excess energy may be easily redistributed among a large number of electronic states.

Acknowledgment. The research reported in this paper has been supported by a grant from the Swedish Natural Science Research Council (NFR), by Project PB97-1377 of the DGES of Spain, and by the European Commission through the TMR Network FMRX-CT96-0079.

References and Notes

(1) Moser, C. C.; Keske, J. M.; Warncke, K.; Farid, R. S.; Dutton, P. L. *Nature* **1992**, *355*, 796.
(2) Gray, H. B.; Winkler, J. R. *Annu. Rev. Biochem.* **1996**, *65*, 537.
(3) Newton, M. D. *Chem. Rev.* **1991**, *91*, 767.
(4) Siegbahn, P. E. M.; Crabtree, R. H. *J. Am. Chem. Soc.* **1997**, *119*, 3103.
(5) Sigfridsson, E.; Ryde, U. *J. Biol. Inorg. Chem.* **1999**, *4*, 99.
(6) Weinkauf, R.; Schanen, P.; Yang, D.; Soukara, S.; Schlag, E. W. *J. Phys. Chem.* **1995**, *99*, 11255.
(7) Weinkauf, R.; Schanen, P.; Metsala, A.; Schlag, E. W.; Bürgle, M.; Kessler, H. *J. Phys. Chem.* **1996**, *100*, 18567.
(8) Weinkauf, R.; Schlag, E. W.; Martinez, T. J.; Levine, R. D. *J. Phys. Chem.* **1997**, *101*, 7702.
(9) Baranov, L.; Schlag, E. W. *Z. Naturforsch* **1999**, *54A*, 387.
(10) Chen, X. G.; Li, P.; Holtz, J. S.; Chi, Z.; Pajcini, V.; Asher, S. A.; Kelly, L. A. *J. Am. Chem. Soc.* **1996**, *118*, 9705.
(11) Pajcini, V.; Chen, X. G.; Bormett, R. W.; Geib, S. J.; Li, P.; Asher, S. A.; Lidiak, E. G. *J. Am. Chem. Soc.* **1996**, *118*, 9716.
(12) McGimpsey, W. G.; Chen, L.; Carraway, R.; Samaniego, W. N. *J. Phys. Chem. A* **1999**, *103*, 6082 and references therein.
(13) Langen, R.; Chang, I. J.; Germanas, J. P.; Richards, J. H.; Winkler, J. R.; Gray, H. B. *Science* **1995**, *268*, 1733.
(14) Hill, R. R.; Jeffs, G. E.; Banaghan, F.; McNally, T.; Werninck, A. R. *J. Chem. Soc., Perkin Trans. 2* **1996**, 1595.
(15) Serrano-Andrés, L.; Fülscher, M. P. *J. Am. Chem. Soc.* **1996**, *118*, 12190.
(16) Serrano-Andrés, L.; Fülscher, M. P. *J. Am. Chem. Soc.* **1996**, *118*, 12200.
(17) McMillin, C. R.; Rippon, W. B.; Walton, A. G. *Biopolymers* **1973**, *12*, 589.
(18) Serrano-Andrés, L.; Fülscher, M. P. *J. Am. Chem. Soc.* **1998**, *120*, 10912.
(19) Demchenko, A. P. *Ultraviolet Spectroscopy of Proteins*; Springer-Verlag: Berlin, 1986.
(20) Robin, M. B. *Higher Excited States of Polyatomic Molecules*; Academic Press: New York, 1975; Vol. II.
(21) Andersson, K.; Malmqvist, P.-Å.; Roos, B. O.; Sadlej, A. J.; Wolinski, K. *J. Phys. Chem.* **1990**, *94*, 5483.
(22) Andersson, K.; Malmqvist, P.-Å.; Roos, B. O. *J. Chem. Phys.* **1992**, *96*, 1218.
(23) Roos, B. O.; Taylor, P. R.; Siegbahn, P. E. M. *Chem. Phys.* **1980**, *48*, 157.
(24) Roos, B. O. *Int. J. Quantum Chem.* **1980**, *S14*, 175.
(25) Roos, B. O.; Fülscher, M. P.; Malmqvist, P.-Å.; Merchán, M.; Serrano-Andrés, L. In *Quantum Mechanical Electronic Structure Calculations with Chemical Accuracy*; Langhoff, S. R., Ed.; Kluwer Academic Publishers: Dordrecht, The Netherlands, 1995; pp 357−438.
(26) Roos, B. O.; Andersson, K.; Fülscher, M. P.; Malmqvist, P.-Å.; Serrano-Andrés, L.; Pierloot, K.; Merchán, M. In *Advances in Chemical Physics: New Methods in Computational Quantum Mechanics*; Prigogine, I., Rice, S. A., Eds.; John Wiley & Sons: New York, 1996; Vol. XCIII, pp 219−331.
(27) Merchán, M.; Serrano-Andrés, L.; Fülscher, M. P.; Roos, B. O. In *Recent Advances in Multireference Theory*; K. H. U., Ed.; World Scientific Publishing Co.: Singapore, 1999; Vol. IV, pp 161−195.
(28) Widmark, P.-O.; Malmqvist, P.-Å.; Roos, B. O. *Theor. Chim. Acta* **1990**, *77*, 291.
(29) Roos, B. O.; Andersson, K.; Fülscher, M. P.; Serrano-Andrés, L.; Pierloot, K.; Merchán, M.; Molina, V. *J. Mol. Struct. (THEOCHEM)* **1996**, *388*, 257.
(30) Malmqvist, P. Å.; Roos, B. O. *Chem. Phys. Lett.* **1989**, *155*, 189.
(31) Mataga, N.; Nishimoto, K. *Z. Phys. Chem.* **1957**, *12*, 335.
(32) Andersson, K.; Blomberg, M. R. A.; Fülscher, M. P.; Karlström, G.; Lindh, R.; Malmqvist, P.-Å.; Neogrády, P.; Olsen, J.; Roos, B. O.; Sadlej, A. J.; Schütz, M.; Seijo, L.; Serrano-Andrés, L.; Siegbahn, P. E. M.; Widmark, P.-O. *MOLCAS*, version 4.0; University of Lund: Lund, Sweden, 1997.
(33) Frisch, M. J.; Trucks, G. W.; Schlegel, H. B.; Scuseria, G. E.; Robb, M. A.; Cheeseman, J. R.; Zakrzewski, V. G.; Montgomery, J. A., Jr.; Stratmann, R. E.; Burant, J. C.; Dapprich, S.; Millam, J. M.; Daniels, A. D.; Kudin, K. N.; Strain, M. C.; Farkas, O.; Tomasi, J.; Barone, V.; Cossi, M.; Cammi, R.; Mennucci, B.; Pomelli, C.; Adamo, C.; Clifford, S.; Ochterski, J.; Petersson, G. A.; Ayala, P. Y.; Cui, Q.; Morokuma, K.; Malick, D. K.; Rabuck, A. D.; Raghavachari, K.; Foresman, J. B.; Cioslowski, J.; Ortiz, J. V.; Stefanov, B. B.; Liu, G.; Liashenko, A.; Piskorz, P.; Komaromi, I.; Gomperts, R.; Martin, R. L.; Fox, D. J.; Keith, T.; Al-Laham, M. A.; Peng, C. Y.; Nanayakkara, A.; Gonzalez, C.; Challacombe, M.; Gill, P. M. W.; Johnson, B. G.; Chen, W.; Wong, M. W.; Andres, J. L.; Head-Gordon, M.; Replogle, E. S.; Pople, J. A. *Gaussian 98*, revision A.5; Gaussian, Inc.: Pittsburgh, PA, 1998.
(34) Deppmeier, B. J.; Driessen, A. J.; Hehre, W. J.; Johnson, J. A.; Klunzinger, P. E.; Lou, L.; Yu, J. *SPARTAN*, version 5.0.3; Wave function Inc.: Irvine, CA, 1997.
(35) Edwards, W. D.; Zerner, M. C. *Theor. Chim. Acta* **1987**, *72*, 347.
(36) Hunt, H. D.; Simpson, W. T. *J. Am. Chem. Soc.* **1953**, *75*, 4540.
(37) Basch, H.; Robin, M. B.; Kuebler, N. A. *J. Chem. Phys.* **1968**, *49*, 5007.
(38) Clark, L. B. *J. Am. Chem. Soc.* **1995**, *117*, 7974.
(39) Moffitt, W. *Proc. Natl. Acad. Sci. U.S.A.* **1956**, *42*, 736.
(40) Bensing, J. L.; Pysh, E. S. *Macromolecules* **1971**, *4*, 659.
(41) Tozer, D. J.; Amos, R. D.; Handy, N. C.; Roos, B. O.; Serrano-Andrés, L.
Mol. Phys. **1999**, *97*, 859.
(42) Serrano-Andrés, L.; Merchán, M.; Rubio, M.; Roos, B. O. *Chem. Phys. Lett.* **1998**, *295*, 195.
(43) Roos, B. O.; Serrano-Andrés, L.; Merchán, M. *Pure Appl. Chem.* **1993**, *65*, 1693.
(44) Roos, B. O.; Fülscher, M. P.; Malmqvist, P.-Å.; Merchán, M.; Serrano-Andrés, L. *Understanding Chem. React.* **1995**, *13*, 357.
(45) Barnes, D. G.; Rhodes, W. *J. Chem. Phys.* **1968**, *48*, 817.
(46) Mommi, R. K.; Urry, D. W. *Macromolecules* **1968**, *1*, 372.